Probability-density function of noise at the output of a two-beam interferometer

Ady Arie* and Moshe Tur

Department of Interdisciplinary Studies, Faculty of Engineering, Tel Aviv University, Ramat Aviv, Tel Aviv, Israel 69978

Evan L. Goldstein

Bellcore, 331 Newman Spring Road, Red Bank, New Jersey 07701-7040

Received December 7, 1990; revised manuscript received June 24, 1991; accepted July 3, 1991

The probability-density function (PDF) of the fluctuating output intensity of a two-beam interferometer, illuminated by a semiconductor laser, is described theoretically and experimentally. The PDF, while dominated by the laser phase noise, may be substantially modified both by the laser intensity noise and by the thermal noise and bandwidth limitations imposed by the detection system. Two regimes of operation are explored. In the coherent regime, for which the interferometer's differential delay τ is much smaller than the laser coherence time τ_c, the form of the PDF is highly sensitive to the mean phase difference between the interfering beams: The PDF is strongly asymmetrical for mean phase differences of 0 and π (experimentally reported here for the first time to our knowledge) but is symmetrical when the interferometer is in quadrature. In the incoherent regime, for which $\tau \gg \tau_c$, the PDF is insensitive to such phase differences. The experimental results are in excellent agreement with a numerical simulation for which it is assumed that the laser phase noise is a Wiener process and for which the finite bandwidth of the detection system, as well as the effects of laser intensity noise and system thermal noise, is taken into account.

1. INTRODUCTION

An optical interferometer translates signal-induced optical phase changes in one of its arms into useful and measurable intensity variations at the interferometer output. But the same interferometric translation process also converts the random phase fluctuations of the light source[1] into output intensity noise that is of major importance in quite a few optical systems.[2-9] While the source phase-induced intensity noise (PIIN) may be used to measure phase-noise-related laser parameters such as the linewidth[2] and the linewidth-enhancement factor,[3] PIIN is more often regarded as a detrimental agent limiting the performance of both analog and digital optical systems.[4-9]

The sensitivity of optical and fiber-optic interferometric sensors is severely degraded by the PIIN, and differential path lengths must be minimized to attain sensitivities in the $\mu\text{rad}/\sqrt{\text{Hz}}$ range. But interference also takes place in optical communications systems containing multiple paths, owing, for example, to (1) Fresnel reflections from optical-fiber connectors,[4,5] (2) Rayleigh backscattering in fibers,[6] and (3) bit-rate limiters.[7] The generated PIIN is always proportional to the incident optical intensity, and, once this intensity is strong enough, PIIN becomes the dominant noise and thereby saturates the signal-to-noise ratio at a level that cannot be improved by feeding more optical power into the system. A similar problem arises in coherent communication systems,[10] in which the relative phase between the source and local oscillator fields fluctuates and results in a power-independent elevated bit error rate.

In the past, PIIN was investigated by studying its mean-square value together with the associated power spectral density.[8,9] While both measures are of considerable value and permit the estimation of pertinent signal-to-noise ratios, they merely represent low-order statistical averages of the noise, and neither of them suffices to determine the complete statistics of the noise. Direct measurement of the probability-density function (PDF) of the PIIN may give much more physical insight into the internal process of phase jumps in lasers.[11-13] To infer the bit error rate achievable in digital optical systems inflicted with PIIN, it is essential to know the PDF. But despite its crucial importance, the PDF has received only limited attention so far. In this paper we explore the form of the PDF of the PIIN at the output of a two-beam interferometer under a variety of conditions ranging from the coherent case, in which the phases of the interfering waves are strongly correlated, to the incoherent one, in which they are statistically independent.

We can obtain the PDF for two-beam interference experimentally by placing a multichannel analyzer at the output of a Mach–Zehnder interferometer. For the incoherent case (for which the relative delay τ imposed by the interferometer is much larger than the source coherence time τ_c), such a measurement was recently reported.[14] However, the coherent case (for which $\tau \ll \tau_c$) has been probed only spottily. In this regime the PDF of PIIN depends quite dramatically on the relative phase $\omega_0\tau$ of the two interfering waves. For $\omega_0\tau = 0$ (i.e., in-phase waves, for which the average output intensity is a maximum), Armstrong[15] theoretically predicted a highly peaked PDF for the coherent case, a function attaining its highest value at the maximum output level of the interferometer with zero values beyond it, but, to our knowledge, no experimental measurements have been reported to verify

0740-3232/91/121936-07$05.00

his model. A similarly shaped PDF, peaked at the minimum output level of the interferometer, is expected for $\omega_0\tau = \pi$, for which the output intensity is a minimum. For $\omega_0\tau = \pi/2$ (phase in-quadrature output, for which interferometric sensors attain their highest sensitivity), Daino *et al.*[16] measured the PDF and reported it to be Gaussian.

The output intensity distributions generated by two-beam interferometers do not depend only on the mean phase difference and degree of phase correlation; they are also strongly influenced by the detection-system bandwidth and by the thermal noise contributed by the detection system. Armstrong[15] assumed infinite detection bandwidth and ignored all noise sources other than PIIN, but these conditions are not met in practice. Experimentally, these effects were studied for an incoherent Mach–Zehnder interferometer.[14] We present here a unified description, both theoretical and experimental, of the intensity PDF generated at the output of a Mach–Zehnder interferometer. Measurements in the coherent regime, obtained for various values of the relative phase, are presented. These are compared with an analytical model that neglects the effects of detection-system bandwidth, source intensity noise, and detector thermal noise. They are also compared with a computer simulation that incorporates all three of these effects. Finally, the simulation results are compared with previously reported PDF measurements obtained in the incoherent regime.[14] While the analytical model alone can only predict the general trends in the observed density functions, the simulation results match the measurements to a high degree.

It should be noted that the problem that we study here is not identical to the one investigated in coherent communication systems.[17–19] In those systems the noise is the result of the filtration of $\exp[i\theta(t)]$, where the random i.f. phase noise $\theta(t)$ is the difference between two independent Wiener processes describing the phase fluctuations of the source and local oscillator. However, at the output of a two-beam interferometer, the noisy quantity of importance is $\exp[i\Delta\phi_\tau(t)]$, where $\Delta\phi_\tau(t) = \phi(t) - \phi(t - \tau)$ is the difference between the source phase noise and its delayed replica. While $\phi(t)$ and $\theta(t)$ are Wiener processes having variances that increase with time, $\Delta\phi_\tau(t)$ is a stationary Gaussian process with a variance that depends only on the interferometer delay τ. It should also be noted that, while Refs. 17–19 model the finite bandwidth of the system by a finite-time integrator, in this paper we assume filters more common in fiber-optic sensors, such as the Butterworth type.

We develop the analytical model in Section 2 and describe the experimental results in Section 3. We compare the measurements with both analysis and computer simulation in Section 4 and present conclusions in Section 5.

2. THEORETICAL BACKGROUND

The output field of a single-mode laser can be written as

$$E(t) = [E_0 + a(t)]\exp[i\omega_0 t + i\phi(t)], \quad (1)$$

where E_0 is the mean field amplitude, ω_0 is the mean angular frequency, $\phi(t)$ is the instantaneous laser phase, and $a(t)$ is the instantaneous deviation of the amplitude from its mean value. After passage through a two-beam interferometer, the output intensity becomes

$$I(t) = \tfrac{1}{2}E_0^2\{1 + \cos[\omega_0\tau + \phi(t) - \phi(t - \tau)]\} + \tfrac{1}{2}E_0[a(t) + a(t - \tau)][1 + \cos(\omega_0\tau)], \quad (2)$$

where τ is the differential delay impressed by the interferometer. In Eq. (2) it is assumed that the intensity is equally divided between the two arms of the interferometer, that the polarizations of the output fields are parallel, and that second-order noise terms are negligible. The expression $\omega_0\tau$, which describes the mean relative phase difference between the interfering waves, determines whether the interferometer's output is minimized [$\omega_0\tau = (2n + 1)\pi$], maximized ($\omega_0\tau = 2n\pi$), or in-quadrature [$\omega_0\tau = (2n + 1/2)\pi$] output. Of the two terms on the right-hand side of Eq. (2), the first represents the PIIN contribution. The second is due to source intensity noise. For $\tau = 0$ the PIIN vanishes, but it rises with τ and, as shown below, becomes dominant even for quite small values of τ/τ_c. Thus, if we neglect the intensity-noise contribution, the fluctuations in Eq. (2) reside entirely in the term $Y_n = \cos[\omega_0\tau + \phi(t) - \phi(t - \tau)]$.

To compute the statistics of Y_n clearly requires knowledge of the statistics of the phase difference $\phi(t) - \phi(t - \tau)$. This process, in turn, can be fairly accurately

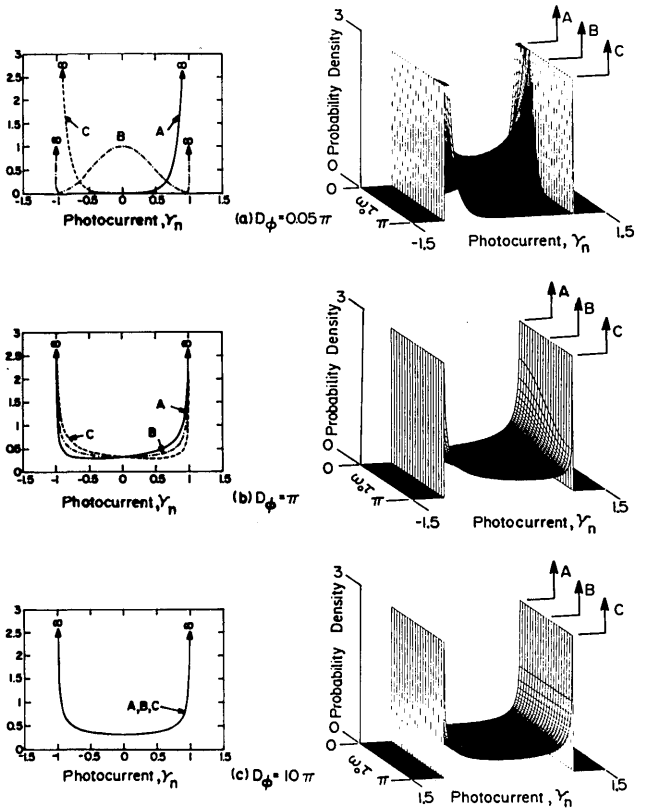

Fig. 1. Theoretical PDF of the normalized PIIN photocurrent $Y_n = \cos[\omega_0\tau + \phi(t) - \phi(t - \tau)]$ at the output of a two-beam interferometer, computed from Eq. (3), for various interferometer settings $\omega_0\tau$ and laser structure functions $D_\phi(\tau)$: (a) coherent regime, $D_\phi(\tau) = 0.05\pi$; (b) intermediate regime, $D_\phi(\tau) = \pi$; (c) incoherent regime, $D_\phi(\tau) = 10\pi$. The three graphs at left represent cross sections of their right-hand counterparts at interferometer settings $\omega_0\tau = 0$ for curve A, $\omega_0\tau = \pi/2$ for curve B, $\omega_0\tau = \pi$ for curve C.

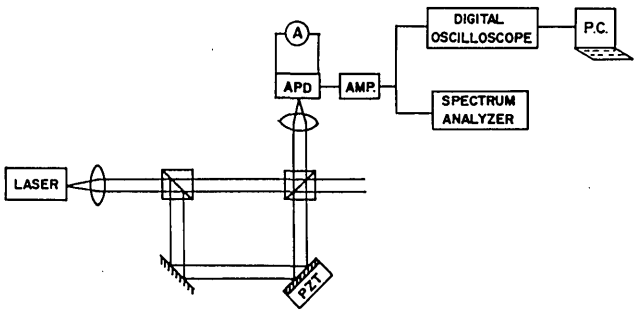

Fig. 2. Experimental setup: A, ammeter; APD, avalanche photodiode; PZT, piezoelectric transducer; AMP., amplifier; P.C., personal computer.

modeled as being zero-mean and Gaussian,[20] since the phase process $\phi(t)$ itself is a random walk whose steps are defined by spontaneous-emission events in the laser.[20] Taking the phase difference to be Gaussian, the laser intensity noise to be negligible, and the detection-system bandwidth to be infinite, we find that the PDF of the normalized output intensity noise Y_n is

$$\mathrm{PDF}(Y_n) = \begin{cases} \dfrac{1}{[2\pi D_\phi(\tau)(1 - Y_n^2)]^{1/2}} \\ \times \displaystyle\sum_{n=-\infty}^{\infty} \left(\exp\left\{ -\frac{[\cos^{-1}(Y_n) - \omega_0\tau + 2\pi n]^2}{2D_\phi(\tau)} \right\} \right. \\ \left. + \exp\left\{ -\frac{[-\cos^{-1}(Y_n) - \omega_0\tau + 2\pi n]^2}{2D_\phi(\tau)} \right\} \right) \\ \qquad -1 < Y_n < 1 \\ 0 \qquad \text{otherwise} \end{cases}, \quad (3)$$

where $D_\phi(\tau) = \langle [\phi(t) - \phi(t - \tau)]^2 \rangle$, sometimes called the phase structure function, is the variance in the phase difference that is accumulated during the interferometer lag time τ. A simpler expression has occasionally appeared in the literature [e.g., Ref. 15, Eq. (5)], but it properly applies only when the interferometer is at maximum ouput ($\omega_0\tau = 2n\pi$).

Figure 1 displays Eq. (3) at various values of $\omega_0\tau$ for interferometers operating in the coherent [Fig. 1(a)], intermediate [Fig. 1(b)], and incoherent [Fig. 1(c)] regimes. Note that all PDF's vanish outside the region $(-1, 1)$, as required by the cosinusoidal character of Y_n. Although the PDF's for Fig. 1 have been clipped at a value of 3, the functions are in fact unbounded for $Y_n = \pm 1$. In the coherent regime [Fig. 1(a)], the PDF clearly depends on the value of $\omega_0\tau$ and exhibits a local peak near $Y_n = \cos(\omega_0\tau)$. In the intermediate state [Fig. 1(b)] the dependence of $\omega_0\tau$ has diminished. In the incoherent regime [Fig. 1(c)], however, the effects of optical path variations in the interferometer are obscured by the large source phase deviations accumulated in time τ; hence the PDF is independent of $\omega_0\tau$.

3. EXPERIMENTAL SETUP AND RESULTS

In order to check Eq. (3) experimentally, we used an AlGaAs semiconductor laser at 847 nm, with a linewidth $\Delta\nu = 40$ MHz and a relaxation frequency of 8 GHz, to illuminate a bulk-optics Mach–Zehnder interferometer (Fig. 2). Using a piezoelectric translator, we adjusted the state $\omega_0\tau$ of the interferometer by slight movements of one mirror. The output light was detected with a fast, variable-gain avalanche photodiode followed by a wideband amplifier and a digitizing oscilloscope. No active stabilization of the interferometer was required, since the measurement time was less than 1 s, whereas the interferometer state remained stable for periods of more than 5 s. The detection-system bandwidth was limited by the oscilloscope to 1 GHz. During each measurement, the scope acquired a sequence of 20,464 8-bit intensity samples $\{I(t), I(t + T), I(t + 2T), \ldots\}$, where T is the delay between samples. These sets of oscilloscope samples were downloaded to a personal computer for data analysis. The interferometer delay τ was determined by measuring the location of the first notch in the output noise spectrum, using a spectrum analyzer. This notch occurs at a frequency $f = 1/\tau$.[9] Since the interferometer's average dc output intensity is of the form $A + B\cos(\omega_0\tau)$, the state of the interferometer could be ascertained by the measurement of the dc current through the avalanche photodiode. The oscilloscope sampling delay T was fixed at 1 μs, considerably longer than both the source coherence time (≈8 ns) and the interferometer's relative delay (which was kept less than 1 ns). Thus the samples may be regarded as statistically independent.[9] Sample 20,464-point se-

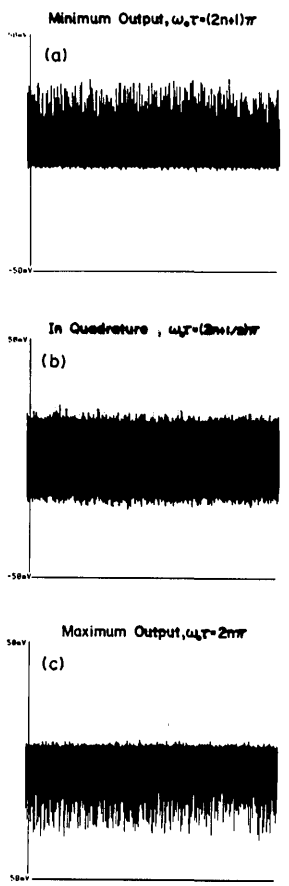

Fig. 3. Intensity sample functions obtained at the output of a Mach–Zehnder interferometer illuminated by a GaAlAs semiconductor laser, with $\tau = 0.5$ ns and sampling interval $T = 1$ μs. Note that the mean intensity $\langle I \rangle$ is blocked by the amplifier; hence these samples do not strictly represent Y_n but rather $Y_n - \langle Y_n \rangle$: (a) minimum output, (b) in-quadrature output, (c) maximum output.

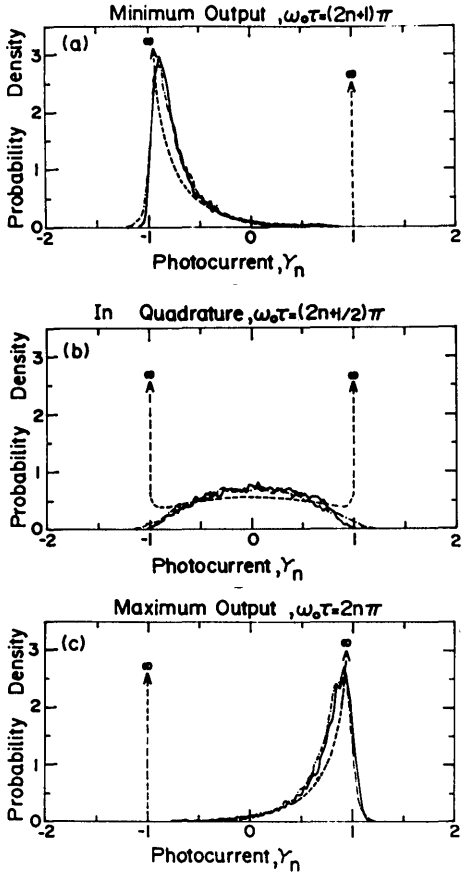

Fig. 4. Experimental (solid curves), theoretical (dashed curves), and simulation (dashed–dotted curves, computed using 32,768 samples) PDF's at the output of a coherent Mach–Zehnder interferometer. Interferometer delay $\tau = 0.5$ ns, sample delay $T = 1$ μs, detection bandwidth $B = 1$ GHz. Theoretical and simulation results were computed by using $D_\phi(\tau) = 0.5$: (a) minimum output, (b) in-quadrature output, (c) maximum output.

quences for the states of minimum, in-quadrature, and maximum output are shown in Fig. 3. As expected, the trace of the minimum setting (maximum setting) is clipped from below (above) by the cosine function. Since the amplifier was ac coupled, these minimum and maximum clipping levels are shifted, which also explains why the trace of the in-quadrature settings does not lie between these two clipping levels. Histograms representing good approximations to the PDF's were directly computed from these sets of sampled intensities. Routinely, we blocked one or both arms of the interferometer and estimated the noise sources other than the PIIN only to show that, in all cases, the PIIN was by far the dominant noise.

The PDF's so obtained for two values of the interferometer delay ($\tau = 0.5$ ns and $\tau = 0.89$ ns) are shown as solid curves in Figs. 4 and 5. Only in the coherent in-quadrature case [Fig. 4(b)], for which the output intensity is approximately equal to $\phi(t) - \phi(t - \tau)$, is the PDF approximately Gaussian. In all other cases the functions are evidently highly non-Gaussian, especially when the interferometer is near its minimum- and maximum-output settings. They also plainly depend on the variance $D_\phi(\tau)$ of the source phase difference accumulated in time τ (cf. Figs. 4 and 5). If the dominant noise source were in fact the laser intensity fluctuations rather than the phase noise, all measured PDF's would be of approximately Gaussian form, since $a(t)$, in Eq. (2), is approximately Gaussian for semiconductor lasers well above threshold[21] when measured over time intervals greater than approximately 10 ps. This effect reinforces the claim that the interferometer output fluctuations are dominated by PIIN. It should be mentioned that, since the wideband amplifier was ac coupled, the mean intensity $\langle I \rangle$ was blocked so that the experiment in fact produced measurements of $Y_n - \langle Y_n \rangle$. For Figs. 4 and 5 we restored the mean value of Y_n by shifting the peak of each measured PDF so it would coincide with the distribution obtained by the numerical simulation to be described in Section 4.

4. DISCUSSION

The dashed curves in Figs. 4 and 5 are plots of Eq. (3), the analytical PDF expression, for various values of $\omega_0\tau$ and D_ϕ. Although the general trends of the analysis are consistent with the measurements, the theoretical expression clearly fails to predict several features of the experimental data. For instance, the theoretical PDF, unlike the measured one, is always zero for normalized intensities outside the interval $[-1, 1]$. Furthermore, for $Y_n = -1$ and $Y_n = 1$, the theoretical density functions become unbounded, whereas the experimental values near the boundaries are not only bounded (as would be expected from a finite-size histogram) but are in fact often quite small. In addition, the theoretical PDF's in the states of minimum and maximum output are mirror images of

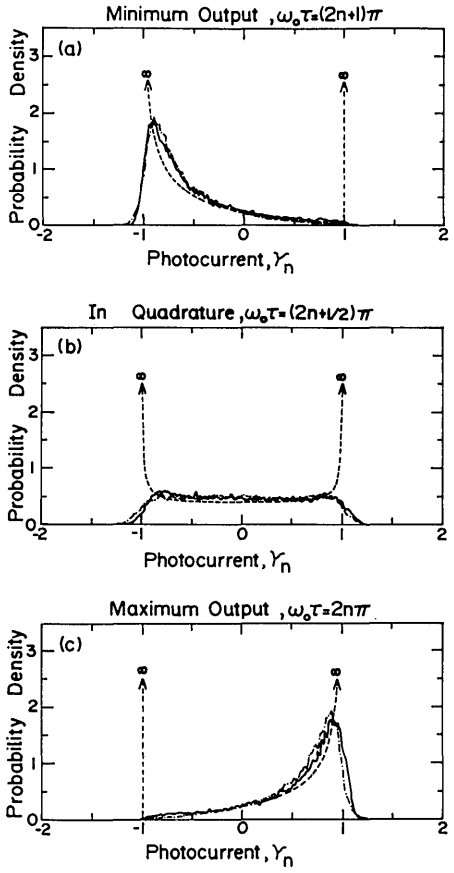

Fig. 5. Same as Fig. 4 but with an interferometer lag time increased to $\tau = 0.89$ ns. For theoretical and simulation results, $D_\phi(\tau) = 1.0$.

each other (with respect to $Y_n = 0$), whereas the peak in the experimental PDF at maximum output is always slightly lower and wider than that at minimum output. As will be shown below, these discrepancies are due in large part to the facts that the theoretical model neglects the source intensity noise, as well as the detector's thermal noise, and that infinite detection-system bandwidth is assumed.

Although we may formally include source intensity noise, thermal noise, and detector-bandwidth limitations in the analytical model, the resulting mathematical expressions are difficult to handle. We have thus examined these effects by incorporating them in a computer simulation that was generated in the following manner. A random-walk process $\bar{\phi}(t)$ was generated with a diffusion rate equal to the phase-noise diffusion rate $[=D_\phi(\tau)/t]$. From it, and from a specified value of $\omega_0\tau$, the simulated random process $\overline{Y}_n = \cos[\omega_0\tau + \bar{\phi}(t) - \bar{\phi}(t-\tau)]$ was computed. A Gaussian pseudorandom variate representing source intensity noise was then added, and the resulting intensity was passed through a seventh-order Butterworth digital filter with a 3-dB bandwidth of 1 GHz. The sample functions so obtained were then charted graphically and yielded an estimate of the PDF of the filtered intensity fluctuations. It should be noted that our simulation incorporates the usual assumption that the laser's frequency noise spectrum is white. This assumption ignores both the laser frequency noise peak near the relaxation-oscillation frequency and the $1/f$ noise. While relaxation oscillations can significantly change the shape of the PIIN spectrum,[9] this is not the case in the current experiments since the laser's relaxation frequency (~8 GHz) greatly exceeded the detector's upper 3-dB frequency (~1 GHz). Also, the low-frequency components of the $1/f$ noise were eliminated by a blocking capacitor. Thus the assumption of white noise is reasonably accurate. This simulation was tested with a bandwidth of 10 GHz, and the laser intensity noise, as well as thermal noise, was ignored. The results accurately reproduce the predictions of Eq. (3).

In order to measure the statistical parameters of the laser intensity noise that were needed in the simulation, we blocked one arm of the Mach–Zehnder interferometer in Fig. 2, so that the laser intensity noise would dominate. We obtained the thermal-noise PDF in a similar fashion by blocking all incident laser light. However, in our experiments this noise component was negligible compared with the intensity-dependent contributions from source intensity noise and the avalanching process in the avalanche photodiode. Thus thermal noise was omitted from the simulation. A set of 20,464 intensity-noise samples was taken with the digitial oscilloscope, and the PDF was constructed. It was found that the PDF of the laser intensity noise is indeed nearly Gaussian, and its standard deviation is proportional to the mean optical intensity. Thus, by measuring the dc output intensity and using this proportionality property, we estimated the normalized variances appropriate for Fig. 4 to be 0.0017 (at minimum ouput), 0.0045 (in quadrature), and 0.0088 (at maximum output). For Fig. 5, the corresponding values were determined to be 0.0016, 0.0032, and 0.0055, respectively.

In order to compare the theoretical results with those of the experiment, one also needs to estimate $D_\phi(\tau)$. Since τ does not greatly exceed the period of our laser's relaxation oscillations and its oscillations are not strongly damped,[20] one cannot simply use the Lorentzian model, $D_\phi(\tau) = 2\pi\Delta\nu\tau$, to calculate the value of the structure function. Instead, we estimated $D_\phi(\tau)$ by choosing a value for $D_\phi(\tau)$ that will produce a best fit between the experimental results and those of the simulation, for example, in the state of in-quadrature output. We got $D_\phi(0.5) = 0.50 \pm 0.03$ (Fig. 4) and $D_\phi(0.89) = 1.0 \pm 0.06$ (Fig. 5).

Finally, an experimental problem that has to be taken into account is the limited accuracy if one brings the interferometer to the minimum and maximum settings. In these states small changes in the differential delay τ are barely observed because the derivative of $\cos(\omega_0\tau)$ is zero for $\omega_0\tau = n\pi$ (for which minimum and maximum output are obtained). A best fit was obtained for $\omega_0\tau = 2\pi + \pi/10$ (maximum output) and $\omega_0\tau = \pi - \pi/10$ (minimum output). These corrections affect the dc output intensity by less than 2.5%.

As is evident from Figs. 4 and 5, the simulation reproduces the experimental measurements quite accurately. Thus, while the PIIN distribution of Eq. (3) indeed accounts for the gross features of the measurements, an accurate PDF prediction in realistic circumstances (as is required, e.g., for error-rate prediction) must incorporate the effects of intensity-noise and bandwidth constraints. These effects modify the predictions of Eq. (3) in several ways:

(1) Smoothing: The intensity-noise (or thermal-noise) Gaussian PDF, when convolved with the PIIN distribution of Eq. (3), causes the overall PDF to have finite values at $Y_n = \pm 1$ and nonzero values outside the interval $[-1, 1]$. The same smoothing may also result from averaging because of the finite measurement bandwidth.

(2) Asymmetry: The standard deviation of the intensity noise is proportional to the average output intensity falling on the detector. Hence, in the coherent regime, more intensity noise is expected at maximum output than at minimum output, which makes the peak near $Y_n = +1$ lower and broader than its counterpart at $Y_n = -1$ [see Eq. (2)].

Figure 6 compares theory, simulation, and experiment for the incoherent regime. The solid curves represent the measurements of Ref. 14. These results were obtained by taking 200,000 photocurrent samples at the output of a Mach–Zehnder interferometer ($\tau \simeq 10$ μs), using a 1.55-μm distributed-feedback laser with a linewidth of 40 MHz, a p-i-n field-effect-transistor receiver (too insensitive to measure the laser intensity noise), and fourth-order rf low-pass filters whose upper 3-dB frequencies were 25 MHz [in Fig. 6(a)] and 1700 MHz [in Fig. 6(b)]. Other than the PIIN, the only measurable source of noise was of thermal origin with Var(thermal)/Var(PIIN) = 0.014.[14] The dashed curves in Fig. 6 are plots of Eq. (3) for $\tau/\tau_c \to \infty$, in which case the result is independent of $\omega_0\tau$. The dashed–dotted curves are the results of the simulation procedure described above, with the use of fourth-order low-pass filter and with the rather small amount of measured thermal noise taken into account. In Fig. 6(b), for which the receiver bandwidth (B) was much larger than the source line-width ($\Delta\nu$), the predic-

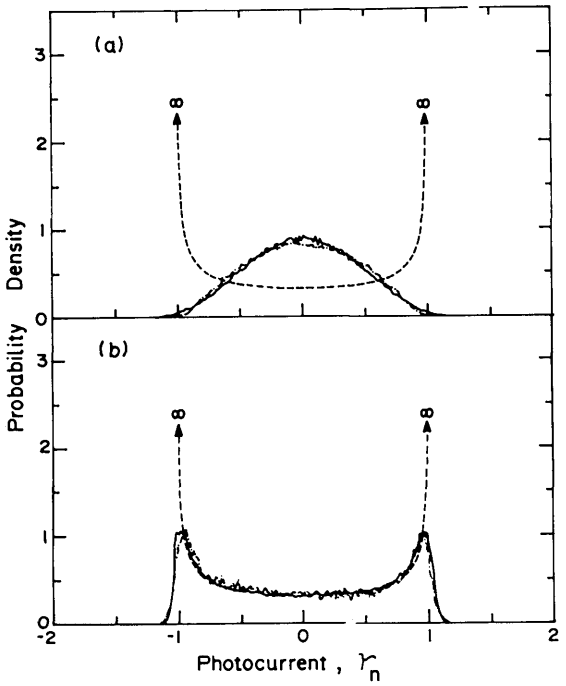

Fig. 6. Experimental (solid curves), theoretical (dashed curves), and simulation (dashed–dotted curves) PDF's at the output of an incoherent Mach–Zehnder interferometer. Interferometer delay $\tau \sim 10$ μs. For simulation and theoretical results, $D_\phi(\tau) = 10$. Detection-system bandwidth B is (a) 25 MHz and (b) 1700 MHz. The simulation graphs were computed by using 1,048,576 samples for (a) and 65,536 samples for (b).

tions of Eq. (3) are quite similar to the measured PDF. Even better agreement is obtained from the simulation. On the other hand, in Fig. 6(a), for which $B/\Delta\nu \simeq 0.6$, the averaging action of the rf filter dominates, and the infinite-bandwidth analysis errs dramatically. In this regime, as is evident from the accuracy of the simulation, PDF predictions must incorporate the effects of the limited detection-system bandwidth. It should be noted that, since in the incoherent regime the average output intensity is always the same, independently of $\omega_0\tau$, the PDF's will retain their symmetry about $Y_n = 0$ even in the presence of intensity noise.

Our simulations for both the coherent and the noncoherent regimes were based on the assumption that the laser phase noise can be described by a Wiener–Levy process. While this model, often referred to as phase-diffusion model, is commonly used in the literature,[20] several other models of phase noise (e.g., the telegraph-noise model[12] and the generalized jump model[13]) also attempt to describe the process of phase fluctuations in lasers. The various models of phase jumps in lasers are usually tested by their ability to predict the correct line shapes of these lasers. However, since the line shape is given by the Fourier transform of the field autocovariance function, it is actually based on the optical field second statistical moment; hence different phase-jump models can sometimes predict the same line shape.[13] Measurement of the PDF of the intensity at the output of a two-beam interferometer may prove to be a more direct and accurate tool to develop and test models that describe the phase fluctuations in lasers.

5. SUMMARY

The probability-density function of the intensity at the output of a two-beam interferometer has been described over the full range of interferometer operation, from coherent to incoherent regimes and from in-phase to in-quadrature and out-of-phase settings. In the coherent regime the PDF depends on the interferometer setting and the laser phase noise but is significantly modified by laser intensity noise, detector thermal noise, and the bandwidth limits of the detector. In the incoherent regime the dependence on the interferometer setting vanishes. The experimental results are in close agreement with a numerical simulation for which we take the phase noise to be a Wiener process and add Gaussian thermal and intensity noise before passing the sum process through a low-pass filter representing the rf bandwidth constraint imposed by the detection system. An analytical model, which accounts for only the laser phase noise and for which an infinite detector bandwidth is assumed, describes the general features of the observed distributions so long as the detection-system bandwidth is considerably larger than the laser linewidth.

These results enable one to predict noise-distribution-dependent quantities such as error probabilities in digital systems corrupted by PIIN. PDF measurements of various lasers can be used to gain insight into the physical process of phase jumps in lasers and to develop accurate statistical models for these phase jumps. Two issues that need further study are the exact shapes of the tails of the PDF's and the effect of the relaxation oscillations when their frequency is within the system rf bandwidth.

ACKNOWLEDGMENT

We thank Ortel corporation for providing the lasers and Eli Raz of Eastronics Israel for providing the digitizing oscilloscope used in this research.

*Present address, Edward L. Ginzton Laboratory, Stanford University, Stanford, California 94305.

REFERENCES

1. A. Dandridge and A. B. Tveten, "Phase noise of single-mode diode lasers," Appl. Phys. Lett. **39,** 530–532 (1981).
2. T. Okoshi, K. Kikuchi, and A. Nakayama, "Novel method for high resolution measurement of laser output spectrum," Electron. Lett. **16,** 630–631 (1980).
3. E. Eichen and P. Melman, "Semiconductor laser lineshape and parameter determination from fringe visibility measurement," Electron. Lett. **20,** 826–828 (1984).
4. J. L. Gimlett, J. Young, R. Spicer, and N. Cheung, "Degradations in Gbit/s DFB laser transmission systems due to phase to intensity noise conversion by multiple reflection points," Electron. Lett. **24,** 406–408 (1988).
5. M. Tur, E. L. Goldstein, and C. A. Brackett, "Bit-error-rate limitations due to laser phase noise in single-mode optical fiber systems with multiple paths," in *OFC '88,* Vol. 1 of OSA 1988 Technical Digest Series (Optical Society of America, Washington, D.C., 1988), paper WQ39.
6. J. L. Gimlett, M. Z. Iqbal, N. K. Cheung, A. Righetti, F. Fontana, and G. Grasso, "Observation of equivalent Rayleigh scattering mirrors in lightwave systems with optical amplifiers," IEEE Photonics Technol. Lett. **2,** 211–213 (1990).
7. M. Tur, E. L. Goldstein, and C. A. Brackett, "Effect of laser noise on a class of bit-rate limiters," Electron Lett. **24,** 126–128 (1988).

8. M. Tur, B. Moslehi, and J. W. Goodman, "Theory of laser phase noise in recirculating fiber optics delay lines," IEEE J. Lightwave Technol. **LT-3,** 20–31 (1985).
9. A. Arie and M. Tur, "Phase induced intensity noise in optical interferometers excited by semiconductor lasers with non-Lorentzian lineshapes," IEEE J. Lightwave Technol. **8,** 1–6 (1990).
10. L. G. Kazovsky, "Impact of laser phase noise on optical heterodyne communication systems," J. Opt. Commun. **7,** 66–78 (1986).
11. A. I. Burshtein, "Kinetics of induced relaxation," Sov. Phys. JETP **21,** 567–573 (1965).
12. J. H. Eberly and K. Wodkiewicz, "Noise in strong laser–atom interactions: phase telegraph noise," Phys. Rev. A **30,** 2381–2389 (1984).
13. A. G. Kofman, R. Zaibel, A. M. Levine, and Y. Prior, "Non-Markovian stochastic jump processes. I. Input field analysis," Phys. Rev. A **41,** 6434–6453 (1990).
14. M. Tur and E. L. Goldstein, "Probability distribution of phase-induded intensity noise generated by distributed-feedback lasers," Opt. Lett. **15,** 1–3 (1990).
15. J. A. Armstrong, "Theory and analysis of laser phase noise," J. Opt. Soc. Am. **56,** 1024–1031 (1966).
16. B. Daino, P. Spano, M. Tamburrini, and S. Piazzolla, "Phase noise and spectral line shape in semiconductor lasers," IEEE J. Quantum Electron. **QE-19,** 263–270 (1983).
17. G. J. Foschini, L. J. Greenstein, and G. Vannucci, "Noncoherent detection of coherent lightwave signals corrupted by phase noise," IEEE Trans. Commun. **36,** 306–314 (1988).
18. G. J. Foschini and G. Vannucci, "Characterizing filtered light waves corrupted by phase noise," IEEE Trans. Inf. Theory **34,** 1437–1448 (1988).
19. I. Garrett, D. J. Bond, J. B. Waite, D. S. L. Lettis, and G. Jacobsen, "Impact of phase noise in weakly coherent systems: a new and accurate approach," IEEE J. Lightwave Technol. **8,** 329–337 (1990).
20. C. H. Henry, "Phase noise in semiconductor lasers," IEEE J. Lightwave Technol. **LT-4,** 298–311 (1986).
21. P. L. Liu, L. E. Fencil, J. S. Ko, I. P. Kaminow, T. P. Lee, and C. A. Burrus, "Amplitude fluctuations and photon statistics of InGaAsP injection lasers," IEEE J. Quantum Electron. **QE-19,** 1348–1351 (1983).